Available online at www.sciencedirect.com
ScienceDirect
Journal of Theoretical Biology 248 (2007) 259–266
Journal of Theoretical Biology
www.elsevier.com/locate/yjtbi

Optimization of interleukin-21 immunotherapeutic strategies

Antonio Cappuccio[1], Moran Elishmereni[1], Zvia Agur*

Institute for Medical Biomathematics (IMBM), P.O.B. 282, Hate'ena St. 10, Bene-Ataroth 60991, Israel

Received 21 December 2006; received in revised form 11 May 2007; accepted 11 May 2007
Available online 18 May 2007

Abstract

The recently discovered interleukin-21 (IL-21) shows strong tumor attenuation in preclinical studies, and is considered a promising cancer immunotherapy agent. Yet, to exploit its potential, therapeutic strategies must be designed to achieve adequate balance between several conflicting aspects. A mathematical model describing the IL-21-antitumor effects provided the basis for application of the optimization methodology, aimed at finding improved immunotherapeutic regimens. Both dosages and inter-dosing intervals were optimized while considering maximal efficacy, determined by reduction of tumor burden, and minimal toxicity, estimated by cumulative IL-21 doses applied. Simulations allowed to compute the optimal regimen and explore its dependence on the weights of the target function. Optimized schedules lead to substantial cancer regression even with relatively low drug concentrations. Collectively, administration times shifted towards treatment onset, and IL-21 intensities sequentially decreased. Interestingly, there was a certain window in which deviations in the total IL-21 dosage administered largely influenced tumor elimination. The findings emphasize the importance of early tumor detection and the critical consequence of the inter-dosing interval on therapeutic efficacy, as supported by similar research involving chemotherapy. Our work provides initial basis for identifying clinically applicable IL-21 therapeutic strategies with improved efficacy/toxicity ratios.

Keywords: Cancer immunotherapy; Cytokine; Efficacy/toxicity ratio; Optimization; Ordinary differential equations

1. Introduction

The design and evaluation of therapeutic regimens that maximize efficacy/toxicity ratios is a critical stage of drug development. However, the identification of adequate treatment strategies is a complicated matter. The wide spectrum of biological reactions induced by a specific therapeutic agent creates an intricate network of processes, thus simple biological intuition may not suffice for designing treatments that fully exploit the potential of a therapeutic agent. Commonly used approaches of experimental trial and error in clinical evaluations are time and resource consuming, with no guarantee of success.

Mathematical models may aid in rational design of drug administration. Such models provide a deeper understanding of the dynamics involved in biological processes, and serve as a basis for implementing mathematical optimization techniques. Over the past 20 years or so, mathematical modeling has been oriented towards rational development and application of cancer treatment (Norton and Simon, 1977; Goldie and Coldman, 1979; Agur et al., 1988, 1992; Ubezio et al., 1994; Kirschner and Panetta, 1998; Skomorovski et al., 2003; Arakelyan et al., 2005; de Pillis et al., 2005, 2006). Optimization algorithms are natural methods within the growing biomathematical tool kit, for studying various aspects of disturbed biological environments. These methodologies have already been applied in the field of cancer chemotherapy (Acharya and Sundareshan, 1984; Swan, 1987, 1988, 1990; Pedreira and Vila, 1991; Swierniak, 1995, 1996; Boldrini and Costa, 2000; Swierniak et al., 2001; Agur et al., 2006) and cancer immunotherapy (de Pillis and Radunskaya, 2001; Burden et al., 2004), with minimization of tumor burden as their primary objective. Such studies have emphasized the importance of adequate selection of therapeutic times,

*Corresponding author. Tel.: +972 3 9733075; fax: +972 3 9733410.
E-mail address: agur@imbm.org (Z. Agur).
[1]These authors contributed equally to this manuscript.

0022-5193/$ - see front matter © 2007 Elsevier Ltd. All rights reserved.
doi:10.1016/j.jtbi.2007.05.015

inter-dosing intervals, and drug intensities, with respect to the final goals.

The newly discovered interleukin-21 (IL-21) was recently suggested as a promising immunotherapeutic agent due to its strong exertion of tumor rejection in a variety of preclinical studies (Ma et al., 2003; Wang et al., 2003; Habib et al., 2003; Moroz et al., 2004; Sivakumar et al., 2004; Nutt et al., 2004). IL-21 enhances tumor kill by facilitating a rapid and efficient transition from innate natural killer (NK) cell responses to adaptive cytotoxic T lymphocyte (CTL) responses, while increasing the natural cytotoxicity of both effector cells. Yet, some immunoinhibitory effects of IL-21 on NK-cells and other factors do exist, creating conflicting processes in IL-21-induced tumor elimination. Moreover, though IL-21-associated toxicities are yet to be evaluated in humans, experience with other cytokine-based therapies suggests that it would clearly be beneficial to limit the use of IL-21 in a clinical scenario. Collectively, the need for accurate balance between stimulatory and inhibitory functions of this cytokine, together with the general preference for minimal drug application, poses an adequate basis for an optimization problem focused on finding administration schedules that fulfill the best compromise. The end effect of such optimized strategies could be advanced response rates in clinical studies of IL-21, accelerated drug development, and improved therapeutic utility.

Mathematical modeling of the anticancerous effects of IL-21 has already given preliminary recommendations for first-stage immunotherapy in primary solid tumors (Cappuccio et al., 2006), suggesting that the tumor immunogenicity is of primary consequence to the chosen immunotherapeutic strategy. The model analysis emphasized the superiority of tumor mass-dependent IL-21 dosing over constant drug administration in aggressive, poorly immunogenic cancers (Cappuccio et al., 2006). In this work, we further refine the suggestions of the previous model by optimizing IL-21 immunotherapy in a murine melanoma model. Various possibilities of treatment regimens, each complying with different therapeutic considerations involving tumor mass and drug toxicity, are explored. The optimization method provides rational and quantitative administrative plans for initial IL-21 immunotherapy, constituted by sequences of administration times and dose intensities. Our analysis supports initiation of IL-21 administrations during the early stages of tumor challenge, and shows that optimal schedules can result in successful reductions of the tumor burden even with relatively low dosages of the immunotherapeutic drug.

2. Methods

2.1. Biological background

The basis for the optimization problem associated with potential IL-21 therapy stems from our recently described mathematical model of the IL-21-antitumor effect (Cappuccio et al., 2006). IL-21 mediates the transition from innate to adaptive anticancer responses, as manifested by the decrease in NK-cell availability coupled with enhancement of tumor-specific $CD8^+$ T-cell expansion and survival. An adequate balance between the two arms of immunity, ultimately determining the efficiency of the response, is a direct consequence of the IL-21 administration strategy. Accordingly, we utilize the optimization approach to find IL-21 dosing schedules that lead to improved tumor eradication. Concurrent with the fact that the immune balance is even more important in aggressive cancers classified with poor immunogenicity, where the NK-cell-mediated tumor lysis plays a central role in eliminating the cancer, simulations are conducted with reference to a non-immunogenic B16 melanoma line for which the previous mathematical model was fitted (Cappuccio et al., 2006).

The implemented method is aimed mainly at minimizing tumor size. Notwithstanding, a toxicity limitation of the immunotherapeutic treatment is taken into account. Although there are indications of only moderate IL-21-induced toxicity in mice (Ma et al., 2003; Wang et al., 2003; Sivakumar et al., 2004), we assume that such a limitation is clinically relevant, as rationalized by a few considerations: First, IL-21 may cause severe inflammation, as it exerts its cytotoxic effects by increasing immune cell-produced molecules such as perforin and granzymes, that cause cell lysis by membrane pore formation or specific intracellular signaling (Cappuccio et al., 2006; Sivakumar et al., 2004; Ma et al., 2003). IL-21 also shares structural and functional homology with IL-2, the dose-limiting side effects of which are known in humans (Wang et al., 2003; Habib et al., 2003; Sivakumar et al., 2004). Accordingly, the optimization goal of tumor size will be considered with, or without, a measure of IL-21-induced cytotoxicity. The latter is mathematically described by a general cytotoxic factor, which accounts for the collective effect of the above-described cytolytic molecules secreted by NK- and $CD8^+$ T-cells in the IL-21 scenario, and estimated in arbitrary units (Cappuccio et al., 2006). This component of the model will therefore be used to estimate the IL-21-associated toxicity.

2.2. Optimization algorithm and simulation settings

The generic ODE system on which the optimization is based is given by

$$\dot{X} = f(X(t)) + \upsilon(t), \tag{1}$$

where $X \in \Re^n$ is the vector of populations, f represents the dynamics, and $\upsilon(t)$ is the control function, acting only on the component X_D $(1 \leqslant D \leqslant n)$. We consider treatment schedules consisting of a finite number of r instantaneous injections at times t_i, represented by control functions $\upsilon(t)$

of the form

$$\upsilon(t) = \left(\overbrace{0, \ldots, \sum_{1}^{r} \upsilon_i \delta(t - t_i)}^{D}, 0, \ldots, 0 \right) = \left(\sum_{1}^{r} \upsilon_i \delta(t - t_i) \right) \mathbf{e}_D. \quad (2)$$

Here, $\delta(\cdot)$ denotes the Dirac delta function, $\mathbf{e}_D = (\overbrace{0, \ldots, 1}^{D}, 0, \ldots, 0)$ is the Dth vector of the standard $\Re^n$ basis, and υ_i is the amount of drug delivered at time t_i.

Next, the space of schedules S of duration T is defined as the set of $2r$-vectors, $s = (t_1, \ldots, t_r; \upsilon_1, \ldots, \upsilon_r)$, satisfying the constraints

$$0 < t_1 < t_2 - \gamma < \cdots < t_r - \gamma < t_r < T, \quad \upsilon_i > 0. \quad (3)$$

Parameter γ is a positive number that represents the minimal interval between two consecutive injections. This is set to avoid clustering of multiple injections, ensuring that the optimized schedules comply with clinical requirements.

Any element $s \in S$ generates a trajectory that is to be denoted by X^s. In our system, the population vector X has six components, $X = (u, x, y, z, p, m)$, accounting for the densities of the drug IL-21, NK-cells, $CD8^+$ T-cells, tumor surface, a memory component, and cytotoxic mediator, respectively, as described in our previous work (Cappuccio et al., 2006) and summarized in Appendix A. Importantly, the analysis considers the surface of the tumor, rather than tumor cell number, as motivated by experimental considerations (Cappuccio et al., 2006). The control function υ is set to act on the first component of X, that is, $D = 1$.

In conjunction with the above-described goals, the following cost function is introduced:

$$\Phi(X^s) = az(T) + b \int_0^T p(\tau)\, d\tau + c \sum_{k=1}^{r} \times \left(\frac{1}{(t_{k+1} - t_k - \gamma)^2} + \frac{1}{V_k^2} \right). \quad (4)$$

The first term represents the tumor surface when therapy ends, while the second term is an indicator of drug-induced toxicity, being proportional to the average concentration of the cytotoxic mediator p (see Appendix A, Eq. (A.5)). The third term ensures that the regimens comply with the constraints in expression (3). Parameters a, b, and c represent the weights of the combination.

The optimal schedules $s^\star$ are designated as the solutions to the problem

$$\Phi(X^{s^\star}) = \min_{s \varepsilon S} \Phi(X^s). \quad (5)$$

These solutions are computed through a steepest descent algorithm, selected for its implementation simplicity, and due to the smoothness of the model. The steepest descent is based on a first order approximation of the derivatives of the performance criterion in Eq. (4). The optimization scheme and numerical methods implemented for our simulations are elaborated in Appendix B.

Model parameters for simulation are configured with respect to preclinical settings and are biologically relevant, as previously shown (Cappuccio et al., 2006) and detailed below (see Appendix A). Concurrent with the fact that the mathematical model depicts initial, short-term immunotherapy in primary tumors (Cappuccio et al., 2006), the considered time window T is confined to 30 days following tumor challenge. The minimal interval between injections, γ, is set to 0.1 days.

The optimization procedure was initialized with a clinically feasible treatment schedule consisting of $r = 10$ injections, each containing 500 ng/ml of IL-21 and equally distributed across a 20-day therapeutic window. For procedures aimed at maximizing tumor mass, simulations were initialized with delayed treatment schedules, in order to allow maximal tumor progression. These consisted of 10 equally distributed 500 ng/ml doses applied during the last 10 days of the considered time frame. The inoculated tumor burden at time 0 was set at 10^5 cells, corresponding to a primary tumor surface of 0.1 mm^2 (Cappuccio et al., 2006).

To compare distinct therapeutic scenarios, simulations were divided into two classes: in the first case, the tumor mass $z(T)$ alone was minimized while optimizing only the administration timing, as implemented by setting $a \neq 0$, $b = 0$, $c \neq 0$. In the second case, minimization of the total objective function (Eq. (4)) was done while optimizing both the timing and the amount of each injection, as set by $a \neq 0$, $b \neq 0$, $c \neq 0$.

3. Results

3.1. Optimizing IL-21 administration times

We first applied the optimization method to search for the best time schedule to satisfy minimal tumor mass, while keeping all dosages at a fixed amount. Accordingly, the procedure was initiated with a schedule of 10 IL-21 injections (500 ng/ml each) within 20 days, and the weights of the cost function were set to $a = 1$, $b = 0$, $c = 0.01$. The final tumor mass decreased monotonically as a function of steepest descent iterations (Fig. 1), proving the efficacy of the optimization procedure. The algorithm required 1820 iterations to convergence within the considered fractional tolerance of 10^{-4}. The time optimization resulted in a final tumor surface of $z_{min}(T) = 0.02$ mm^2, which was approximately 20% of the initial value (Fig. 2, left panel). The injection times during the optimization were globally shifted toward the initial days of tumor challenge therapy beginning 0.09 days after inoculation (Fig. 2, right panel). The first two injections were separated by a minimal interval of 1.8 days, while the last two injections were

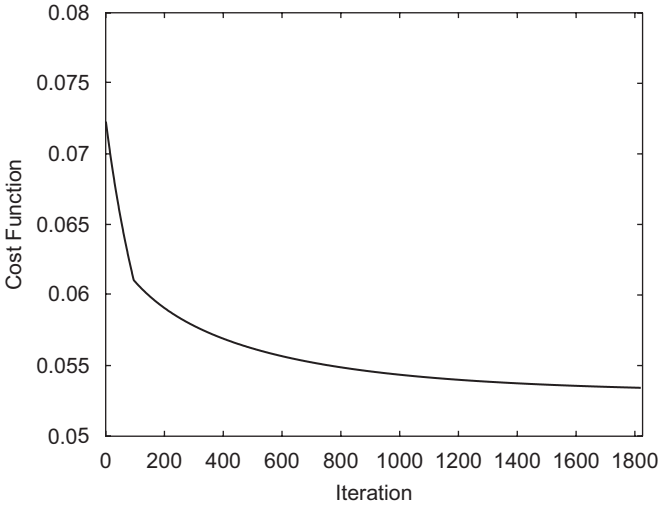

Fig. 1. Gradual decrease of final tumor mass during optimization. An initial treatment schedule, including ten 500 ng/ml IL-21 injections equally distributed across a 20-day therapeutic window, was optimized to ensure a minimal tumor size following therapy. Cost function weights were set to $a = 1$, $b = 0$, $c = 0.01$. The final tumor mass, that is the focus of the cost function, is displayed with respect to the optimization iterations.

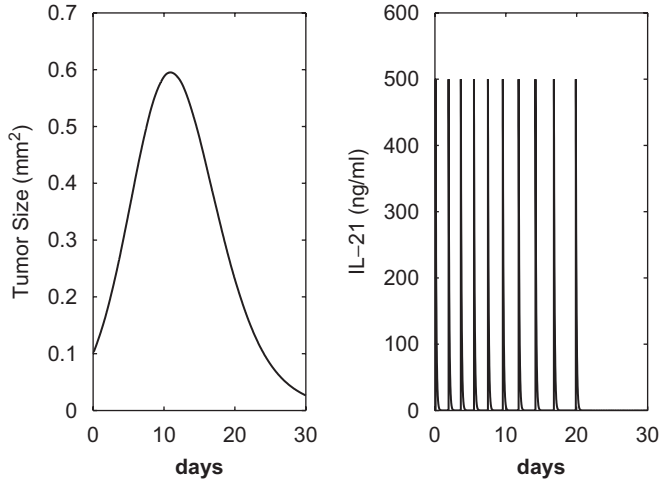

Fig. 2. Optimization of IL-21 administration times to achieve minimal tumor mass. An initial treatment regimen, consisting of ten 500 ng/ml IL-21 injections equally distributed across a 20-day therapeutic window, was optimized with the purpose of achieving the minimal tumor size at therapy termination. Cost function weights were set to $a = 1$, $b = 0$, $c = 0.01$. The optimized treatment schedule (right panel) is displayed alongside its resulting tumor dynamics (left panel).

separated by the maximal distance of about 3.1 days. These results emphasize that the earliest stage of the treatment, when the tumor mass is still minor, is the most crucial one.

A comparison of the performance of an optimal regimen to the outcome of alternative choices allows to assess the impact of the optimization procedure and test its efficacy in a specific setting. Ideally, the optimization would prove to be advantageous if the optimal strategy results in a tumor mass vastly lower than the one obtained by the worst possible therapeutic regimen. It was therefore important to compare the above-evaluated z_{min} (Fig. 2), signifying the best response to therapy, with the largest final tumor mass, z_{max}. This problem was formulated by applying the weights $a = -1$, $b = 0$, $c = 0.01$ to the cost function. Since maximal tumor masses can be generated by a late treatment onset, we used an initial regimen which was similar in drug intensity, but delayed (i.e. ten 500 ng/ml injections distributed at the last 10 days of the 30-day time frame). Indeed, the cost function drastically decreased during optimization (Fig. 3, left panel), requiring only 400 iterations to convergence. Injection times were shifted toward the late stage of the therapeutic window (Fig. 3, right panel), creating an optimized schedule commencing at day 23, and terminating at day 29 following tumor challenge (Fig. 4, right panel). A value of $z_{max}(T) \simeq 200\,\mathrm{mm}^2$ was obtained (Fig. 4, left panel), a 10^4-times larger tumor than $z_{min}(T)$. The maximization of the final tumor mass confirmed the strong influence of the optimization procedure, as the selected therapeutic time schedule drastically affected the treatment outcome within the considered time span.

3.2. Optimizing IL-21 administration times and dosages

Next, both the times and dosages of IL-21 application were optimized in relation to the extended cost, described by Eq. (4). In the first case, cost function weights were set to $a = 1$, $b = 10^{-4}$, $c = 0.01$, simulating a weak influence of the IL-21 dosage and a strong influence of the final tumor mass on the cost function. After 2115 iterations, a final tumor size of $0.01\,\mathrm{mm}^2$, equivalent to 10% of the initial tumor burden, was obtained (Fig. 5, left panel), with a total

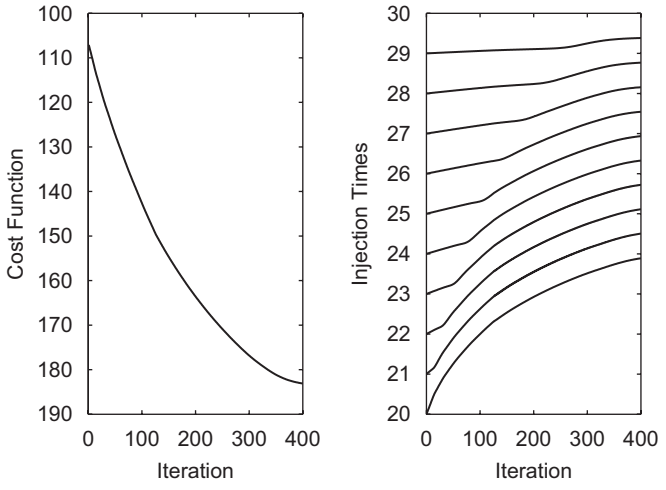

Fig. 3. Gradual increase of final tumor mass and modification of IL-21 administration times during optimization. An initial treatment regimen, consisting of ten 500 ng/ml IL-21 injections from day 20 to 29, was optimized with the purpose of achieving maximal tumor size at the end of therapy. Cost function weights were set to $a = -1$, $b = 0$, $c = 0.01$. The final tumor mass, that is the focus of the cost function (left panel), as well as the shifting time schedule for IL-21 application (right panel), is displayed as a function of the optimization iterations.

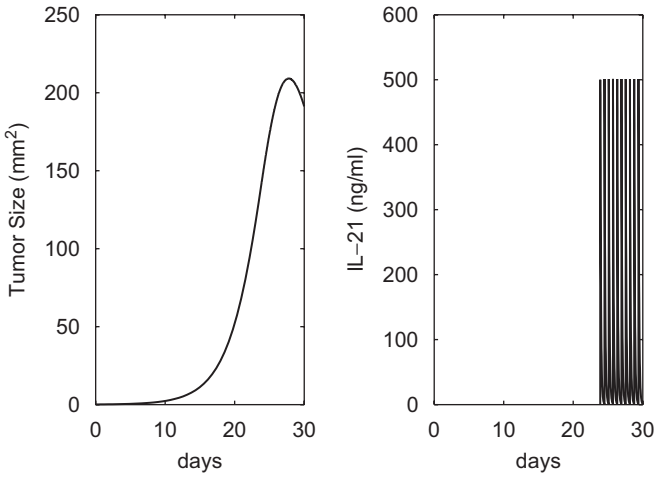

Fig. 4. Optimization of IL-21 administration times to achieve maximal tumor mass. An initial treatment regimen, consisting of ten 500 ng/ml IL-21 injections from day 20 to 29, was optimized with the purpose of achieving the maximal tumor size at the end of therapy. Cost function weights were set to $a = -1$, $b = 0$, $c = 0.01$. The optimized treatment schedule (right panel) is displayed alongside its resulting tumor dynamics (left panel).

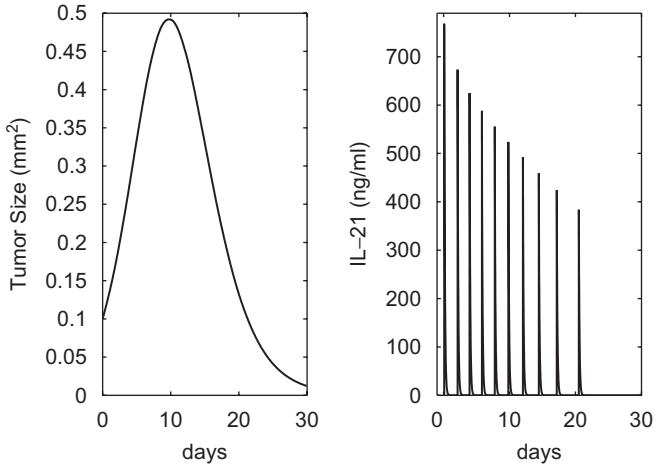

Fig. 5. Optimization of IL-21 administration times to minimal tumor mass, with low consideration of toxicity. An initial treatment regimen, consisting of ten 500 ng/ml IL-21 injections equally distributed across a 20-day therapeutic window, was optimized with the purpose of minimizing tumor burden as well as drug toxicity. An indicator of IL-21 treatment toxicity was introduced as a low weight factor in the objective function, by setting the cost function weights at $a = 1$, $b = 10^{-4}$, $c = 0.01$. The optimal treatment schedule (right panel) is displayed alongside its corresponding tumor dynamics (left panel).

concentration of IL-21 that amounted to 5490 ng/ml. As in the previous case, injection times collectively tended to the initial stages of tumor challenge. Interestingly, dose intensities spread across several values, decreasing toward termination of therapy (Fig. 5, right panel). Thus, by allowing the drug amounts to be optimized with low weight of toxicity, we achieved a schedule that was more efficient in reducing tumor mass, but that required higher total IL-21 dosages.

To investigate how the optimized treatment changes in function of the weights of the target, parameter b was increased from 10^{-4} to 5×10^{-4}, enhancing the contribution of the total IL-21 applied, or the total cytotoxic factor produced. Here, following 2232 iterations, optimized injection times were not significantly modified as compared to the previous case, and dosages remained monotonically decreasing, yet applied IL-21 intensities were all lower (Fig. 6, right panel). In these conditions, the final tumor mass arrived at 0.03 mm^2 (Fig. 6, left panel), with a therapeutic schedule involving a total IL-21 dosage of 4445 ng/ml. Thus, this strategy seemed superior to the regimen optimized with respect to time alone (Fig. 2), the latter requiring a higher drug quantity (5000 ng/ml) to reach a slightly lower final tumor mass. This exemplifies that an adequate tumor reduction can be achieved with lower amounts of IL-21, provided that the doses are calibrated according to their optimal values.

The IL-21 dose intensities maintained a monotonically decreasing pattern throughout the optimized schedule (Fig. 7, right panel), even when the relative impact of the drug toxicity on the cost function was elevated further ($b = 3.45 \times 10^{-3}$). However, a significantly lower total IL-21 dose of 2740 ng/ml was achieved via this strategy, as observed after 2357 iterations. The resulting tumor size after 30 days was in this case 0.18 mm^2, a higher value than the initial tumor mass (Fig. 7, left panel), indicating that there is a basal amount of drug necessary to promise successful therapy within the considered time window.

To further elucidate the relationship between the final tumor mass and the total amount of IL-21 administered during treatment, we ran simulations with steadily

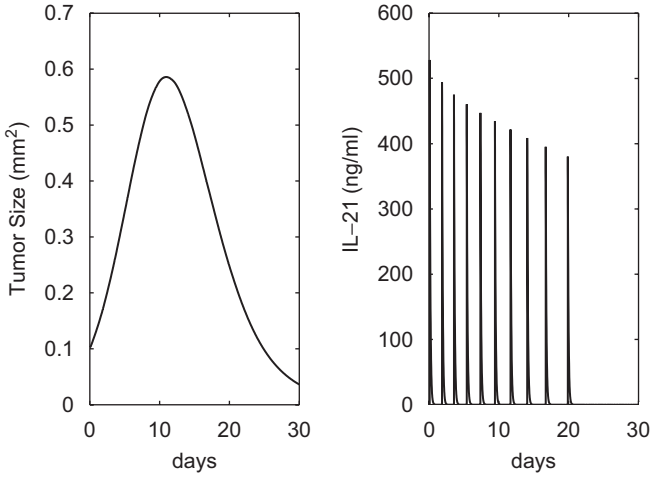

Fig. 6. Optimization of IL-21 administration times to minimal tumor mass, with moderate–high consideration of toxicity. An initial treatment regimen, consisting of ten 500 ng/ml IL-21 injections equally distributed across a 20-day therapeutic window, was optimized with the purpose of minimizing tumor burden as well as drug toxicity. An indicator of IL-21 treatment toxicity was introduced as a moderate–high weight factor in the objective function, by setting the cost function weights at $a = 1$, $b = 5 \times 10^{-4}$, $c = 0.01$. The optimal treatment schedule (right panel) is displayed alongside its corresponding tumor dynamics (left panel).

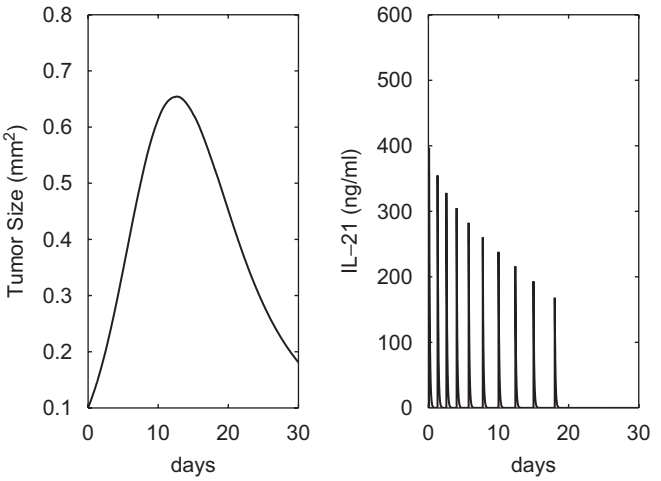

Fig. 7. Optimization of IL-21 administration times to minimal tumor mass, with high consideration of toxicity. An initial treatment regimen, consisting of ten 500 ng/ml IL-21 injections equally distributed across a 20-day therapeutic window, was optimized with the purpose of minimizing tumor burden as well as drug toxicity. An indicator of IL-21 treatment toxicity was introduced as a high weight factor in the objective function, by setting the cost function weights at $a = 1$, $b = 3.45 \times 10^{-3}$, $c = 0.01$. The optimal treatment schedule (right panel) is displayed alongside its corresponding tumor dynamics (left panel).

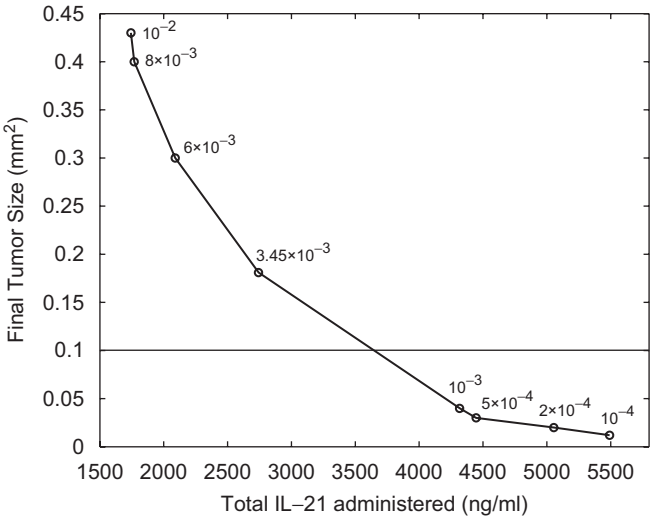

Fig. 8. Hyperbolic correlation between final tumor mass of an optimized regimen and its cumulative IL-21 doses (affected by the toxicity factor weight in the cost function). Several simulations of the optimization method, targeted at minimizing tumor burden as well as drug toxicity, were applied with an increasing significance for the toxicity factor, i.e. an increasing value for b. Each simulation was initiated at a treatment regimen of ten 500 ng/ml IL-21 injections equally distributed across a 20-day therapeutic window. Final tumor mass of each simulation (dots) corresponds to the indicated value of weight b. The horizontal line represents initial tumor size.

increasing values of parameter b. For all simulations, the initial tumor surface amounted to 0.1 mm^2. A hyperbola-like behavior was observed, where increasing levels of drug application (corresponding to decreasing values of b) were coupled with reduced final tumor sizes (Fig. 8). The slope of this curve showed that, for optimized treatment schedules applying a cumulative IL-21 dose between 1700 and 3000 ng/ml, the final tumor sizes resulting from such regimens varied largely, being highly sensitive to the total IL-21 amounts, whereas above this range, a certain saturation effect was detectable.

4. Discussion

The search for rational ways to apply immunotherapeutic agents and to improve their efficacy is of high relevance in medical treatments. Biomathematical models are becoming increasingly instrumental in planning concrete treatment strategies, as they improve our understanding of how the timing of drug administration, the inter-dosing interval, drug fractionation, and other aspects of treatment scheduling may affect the patient. In this work, optimization tools were implemented on the basis of a mathematical model describing the antitumor effects of the cytotoxic agent IL-21, and subsequently allowed to draw a number of clinical implications regarding initial IL-21 immunotherapy for primary cancer.

This use of an optimization method to detect IL-21 regimens minimizing tumor size appears to be theoretically justified: treatment regimens, consisting of a constant number of doses with fixed intensities but different administration times, were shown to produce final tumor sizes varying within a range of four orders of magnitude within the considered time window of 30 days. Thus, the outcome of the therapy strongly depends on the injective times and inter-dosing intervals of the immunotherapeutic agent. These results support previous preclinically validated studies showing that there is a stringent correlation between the efficacy of chemotherapy and the therapeutic interval, and that lower drug doses spaced appropriately enhance treatment success (Agur et al., 1988, 1992; Skomorovski et al., 2003; Ubezio et al., 1994).

The dynamics of the injection times and dosages during the optimization give rise to other interesting insights. In simulations aimed at minimizing tumor mass, administration times moved towards the first stages of tumor challenge, where initial IL-21 injections appeared more influential. This can be rationalized by the following observations: first, the tumor is smaller at the beginning of therapy, hence the antitumor activity is more effective at that stage. In addition, the final time of therapy (T) is considered smaller than the half-life of the cytotoxicity mediator (Cappuccio et al., 2006; Moroz et al., 2004). This implies that early initiation of therapy provides an antitumor effect that would last during the entire time span under consideration. Conversely, the effects of a delayed treatment onset are largely manifested beyond our therapeutic window.

The optimized dosages of IL-21 were within the normative biological range of 200−700 ng/ml each. Optimization of both times and dose intensities results in schedules that were comparable to the case of time

optimization only, with the use of a lower concentration. Specifically for a regimen of 10 IL-21 injections, the final tumor burden achieved by an optimized regimen applying a total IL-21 concentration of 5000 ng/ml was similar to that of a regimen applying 4445 ng/ml. Such differences in drug intensities could be significant in the clinical scenario, since rational application of IL-21 could very well reduce adverse events associated with its use.

Minimization of treatment toxicity was considered in the optimization process by introducing the weight of the IL-21-induced cytotoxic mediator concentration in the cost function. Implementing the optimization with increasing values of this weight consistently leads to optimized regimens with a monotonically decreasing sequence of IL-21 dosages. However, analysis of several optimized regimens generated with respect to different toxicity factor weights revealed a high sensitivity of the final tumor mass only for a total IL-21 dosage within 1700−3000 ng/ml, whereas beyond this range the dependence decreases. These simulations show that the dependence of the optimal schedule upon the specific target function is not straightforward. We emphasize the importance of carefully calibrating the weights with respect to patient-specific clinical requirements, such as diverse toxicity profiles, tumor types, and basal antitumor immunity levels.

Importantly, since the non-convex optimization problem presented in this work is dealt with via local search with single initialization, the obtained schedules may represent only local minima, and global optimization techniques may provide better results. Moreover, with respect to the optimization procedure, the simplistic steepest descent method proved to be satisfactory, yet was not exempt from the well-known feature of slow convergence. Thus, more efficient optimization algorithms may reveal even more beneficial regimens.

The optimization method shown in our work may be adapted to compute optimal strategies in a feedback form, that is, real-time modification of treatment strategies according to actual immunological responses of patients. This is of primary importance for clinical drug development. Indeed, stochastic disturbances and a number of processes, currently not considered in the model, may induce deviations from the deterministic description, emphasizing the need for flexible therapies. Additionally, expansion of the IL-21 model to depict long-term immunotherapy and consideration of secondary tumor challenge and metastatic processes will enable optimization methods to execute clinically relevant simulations and to produce more reliable predictions.

Acknowledgments

The work was supported by a Marie Curie Grant MRTN-CT-2004-503661 (A. Cappuccio) and by the Chai Foundation (Z. Agur and M. Elishmereni).

Appendix A. The mathematical model

The following quantities form the mathematical model (Cappuccio et al., 2006) that serves as the basis of optimization problems described in this work:

1. IL-21 concentration measured in units of ng/ml (u);
2. NK-cells counted in the spleen (x);
3. Specific $CD8^+$ T-cells counted in draining lymph nodes (y);
4. Tumor surface measured in mm^2 (z);
5. Mediator of the NK-cell/$CD8^+$ T-cell cytotoxicity measured in arbitrary units (p);
6. Mediator responsible for the long-term survival of $CD8^+$ T-cells measured in arbitrary units (m).

The system is given by the following equations:

$$\dot{u} = -\mu_1 u, \tag{A.1}$$

$$\dot{x} = r_1 x\left(1 - \frac{x}{h_1(u)}\right), \tag{A.2}$$

$$\dot{y} = r_2 y\left(1 - \frac{y}{h_2(m)}\right), \tag{A.3}$$

$$\dot{z} = g(z) - k_1 pxz - k_2 pyz. \tag{A.4}$$

$$\dot{p} = \frac{\beta_1 u}{\beta_2 + u} - \mu_3 p, \tag{A.5}$$

$$\dot{m} = \alpha u - \mu_2 m, \tag{A.6}$$

where $h_1(u)$ in Eq. (A.2), the carrying capacity of the NK-cells, is a decreasing saturated function of IL-21, as shown by

$$h_1(u) = \frac{p_1 u + p_2}{u + q_1}, \tag{A.7}$$

and $h_2(m)$ in Eq. (A.3), the carrying capacity of specific $CD8^+$ T-cells, is an increasing saturated function of the memory factor m, as given by

$$h_2(m) = h_2(0) + \frac{\sigma m}{1 + m/D}. \tag{A.8}$$

The function $g(z)$ represents the tumor growth law of B16 melanoma in non-treated mice, as formulated by

$$g(z) = r_3 z\left(1 - \left(\frac{z}{K}\right)^{\omega}\right). \tag{A.9}$$

For all simulations in this work, we used the following parameter values, as previously indicated (Cappuccio et al., 2006): $\mu_1 = 10$, $r_1 = 0.095$, $p_1 = 0.01$, $p_2 = 1.054$, $q_1 = 0.54$, $r_2 = 0.26$, $h_2(0) = 0.066$, $\sigma = 0.0071$, $D = 0.19 \times 10^3$, $r_3 = 0.48$, $K = 400$, $\omega = 1.5$, $\beta_1 = 0.1$, $\beta_2 = 0.1$, $\mu_3 = 0.08$, $\alpha = 0.57$, $\mu_2 = 0.014$. The initial condition for all simulations was $[0, h_1(0), h_2(0), 0.1, 0, 0]$, representing an untreated scenario in which tumor growth is unchallenged by the immune system (Cappuccio et al., 2006).

Appendix B. Numerical methods

The optimal regimens presented in this work were computed through an implementation of the gradient method, combined with a line search. At each iteration of the steepest descent, the cost function was evaluated via a fourth order Runge–Kutta integrator of the system (as shown in Appendix A, Eqs. (A.1)–(A.8)) in $[0, T]$, with the specified initial conditions. The partial derivatives of the cost function in Eq. (4) were approximated by the finite differences

$$\frac{\partial \Phi(X^s)}{\partial s_i} \simeq \frac{\Delta \Phi(X^s)}{\Delta s_i} = \frac{\Phi(X^{s+he_i}) - \Phi(X^s)}{h} \tag{B.1}$$

for $i = 1, \ldots, 2r$. Here, s_i represents the ith component of the schedule $s = (t_1, \ldots, t_r; \upsilon_1, \ldots, \upsilon_r)$, and the step h was set to 10^{-3}.

All numerical procedures applied were implemented via *matlab* programming. Specifically, the equations were solved using the function *ode45*, and the line search was executed via the routine *fmin*. A fractional convergence tolerance of 10^{-4} was applied as the arrest condition of the steepest descent.

References

Acharya, R., Sundareshan, M., 1984. Development of optimal drug administration strategies for cancer-chemotherapy in the framework of systems theory. Int. J. Biomed. Comput. 15 (2), 139–150.

Agur, Z., Arnon, R., Schechter, B., 1988. Reduction of cytotoxicity to normal tissues by new regimens of phase-specific drugs. Math. Biosci. 92, 1–15.

Agur, Z., Arnon, R., Schechter, B., 1992. Effect of the dosing interval on myelotoxicity and survival in mice treated by cytarabine. Eur. J. Cancer 28A (6–7), 1085–1090.

Agur, Z., Hassin, R., Levi, S., 2006. Optimizing chemotherapy scheduling using local search heuristics. Oper. Res. 54 (5), 829–846.

Arakelyan, L., Merbl, Y., Agur, Z., 2005. Vessel maturation effects on tumour growth: validation of a computer model in implanted human ovarian carcinoma spheroids. Eur. J. Cancer 41 (1), 159–167.

Boldrini, J., Costa, M., 2000. Drug resistance, therapy burden and optimal treatment regimen for cancer chemotherapy. IMA J. Math. Appl. Med. Biol. 17, 33–51.

Burden, T., Ernstberger, J., Fister, R., 2004. Optimal control applied to immunotherapy. Discrete Continuous Dyn. Syst. Ser. B 4 (1), 135–146.

Cappuccio, A., Elishmereni, M., Agur, Z., 2006. Immunotherapy by IL-21: potential treatment strategies evaluated in a mathematical model. Cancer Res. 66 (14), 7293–7300.

de Pillis, L., Radunskaya, A., 2001. A mathematical tumor model with immune resistance and drug therapy: an optimal control approach. J. Theor. Med. 3, 79–100.

de Pillis, L., Radunskaya, A., Wiseman, C., 2005. A validated mathematical model of cell-mediated immune response to tumor growth. Cancer Res. 65 (17), 7950–7958.

de Pillis, L., Gu, W., Radunskaya, A., 2006. Mixed immunotherapy and chemotherapy of tumors: modeling, applications and biological interpretations. J. Theor. Biol. 238 (4), 841–862.

Goldie, J., Coldman, A., 1979. A mathematical model for relating the drug sensitivity of tumors to their spontaneous mutation rate. Cancer Treat. Rep. 63, 1727–1733.

Habib, T., Nelson, A., Kaushansky, K., 2003. IL-21: a novel IL-2-family lymphokine that modulates B, T, and natural killer cell responses. J. Allergy Clin. Immunol. 112 (6), 1033–1045.

Kirschner, D., Panetta, J., 1998. Modeling immunotherapy of the tumor–immune interaction. J. Math. Biol. 37 (3), 235–252.

Ma, H., Whitters, M., Kontz, R., Senices, M., Young, D., Grusby, M., Collins, M., Dunussi-Joannopoulos, K., 2003. IL-21 activates both innate and adaptive immunity to generate potent antitumor responses that require perforin but are independent of ifn-gamma. J. Immunol. 171 (2), 608–615.

Moroz, A., Eppolito, C., Li, Q., Tao, J., Clegg, C., Shrikant, P., 2004. IL-21 enhances and sustains CD8+ t cell responses to achieve durable tumor immunity: comparative evaluation of IL-2, IL-15, and IL-21. J. Immunol. 173 (2), 900–909.

Norton, L., Simon, R., 1977. Tumor size, sensitivity to therapy, and design of treatment schedules. Cancer Treat. Rep. 61, 1307–1317.

Nutt, S., Brady, J., Hayakawa, Y., Smyth, M., 2004. Interleukin 21: a key player in lymphocyte maturation. Crit. Rev. Immunol. 24 (4), 239–250.

Pedreira, C., Vila, V., 1991. Optimal schedule for cancer chemotherapy. Math. Program. 52, 11–17.

Sivakumar, P., Foster, D., Clegg, C., 2004. Interleukin-21 is a T-helper cytokine that regulates humoral immunity and cell-mediated anti-tumour responses. Immunology 112 (2), 177–182.

Skomorovski, K., Harpak, H., Ianovski, A., Vardi, M., Visser, T., Hartong, S., van Vliet, H., Wagemaker, G., Agur, Z., 2003. New TPO treatment schedules of increased safety and efficacy: pre-clinical validation of a thrombopoiesis simulation model. Br. J. Haematol. 123 (4), 683–691.

Swan, G., 1987. Optimal control analysis of a cancer chemotherapy problem. J. Math. Appl. Med. Biol. 4, 171–184.

Swan, G., 1988. General applications of optimal control theory in cancer chemotherapy. IMA J. Math. Appl. Med. Biol. 5 (4), 303–316.

Swan, G., 1990. Role of optimal control theory in cancer chemotherapy. Math. Biosci. 101 (2), 237–284.

Swierniak, A., 1995. Cell cycle as an object of control. J. Biol. Syst. 3, 41–54.

Swierniak, A., 1996. Optimal control problems arising in cell-cycle-specific cancer chemotherapy. Cell Prolif. 29, 117–139.

Swierniak, A., Ledzewicz, U., Schattler, H., 2001. Optimal control for a class of compartmental models in cancer chemotherapy. J. Theor. Med. 3, 79–100.

Ubezio, P., Tagliabue, G., Schechter, B., Agur, Z., 1994. Increasing 1-β-D-arabinofuranosylcytosine efficacy by scheduled dosing intervals based on direct measurement of bone marrow cell kinetics. Cancer Res. 54, 6446–6451.

Wang, G., Tschoi, M., Spolski, R., Lou, Y., Ozaki, K., Feng, C., Kim, G., Leonard, W., Hwu, P., 2003. In vivo antitumor activity of interleukin 21 mediated by natural killer cells. Cancer Res. 15 (63), 9016–9022.